# Technology of fabrication of $CDS_XTe_{1-X}$ solid solution on silicon substrate

*I. B.* Sapaev[1*], *B.* Sapaev[2], and *D.* Babajanov[3]

[1]"Tashkent Institute of Irrigation and Agricultural Mechanization Engineers" National Research University, Tashkent, Uzbekistan
[2]Tashkent State Agrarian University, Tashkent, Uzbekistan
[3]Tashkent State University of Economics, Tashkent Uzbekistan

**Abstract**. Heterojunction between Si and $CdS_xTe_{1-x}$ have been obtained by vacuum deposition of powders of cadmium sulfide and cadmium telluride on the surface of monocrystalline silicon. The optimal temperature regime for the growth of the $CdS_xTe_{1-x}$ solid solution on the silicon surface has been determined. The values of the crystal lattice constant and the thickness of the $CdS_xTe_{1-x}$ solid solution at the interface of the n/Si – n/ $CdS_xTe_{1-x}$ heterostructure are calculated.

## 1 Introduction

Obtaining a heterojunction based on silicon (Si) [1,2] and $A^2B^6$ [3,4], and $A^3B^5$ semiconductor compounds is of scientific and practical interest. This would allow more efficient use of the potential capabilities of the silicon with $A^2B^6$ and $A^3B^5$ semiconductor compounds in solid-state electronics, photovoltaics, and photovoltaic energy. In this work, certain design issues in the technology of obtaining an efficient heterojunction based on Si and cadmium telluride CdTe without surface states are considered. However, it is known [5] that the crystal lattice constant of silicon (α = 5.43Å) and cadmium telluride CdTe (α = 6.477Å) differ considerably; therefore, to create an effective heterojunction between these semiconductor materials, it is necessary to use an intermediate semiconductor material that would match their crystal lattice constants. Such a material can be a $CdS_xTe_{1-x}$ solid solution (SS), which is continuous, and its lattice constant changes from α = 5.84Å in cadmium sulfide to α = 6.477Å in cadmium telluride. In this solid solution, one can find a composition in which the lattice constant would correspond to the lattice constant of silicon. For this purpose, $CdS_xTe_{1-x}$ solid solutions of various compositions were formed on the silicon surface. For this purpose, CdS and CdTe powders in a weight ratio of 10:1 were placed in a quartz crucible and sprayed onto the silicon surface in a vacuum of $10^{-5}$torr. In this case, the source - the crucible was heated in the aisles to $950^0$C - $1100^0$C, and the substrate (Si) was at a temperature of 150-$250^0$C.

*Corresponding author: sapaevibrokhim@gmail.com

## 2 Methods

We created n/Si – n/$CdS_xTe_{1-x}$ heterojunctions by sputtering indium in the vacuum of $\sim 10^{-5} Torr$ with a thickness of ~ 400-500Å on the surface of high-resistance n-type films with a resistivity of $\rho \approx 10^5 - 10^6 \Omega \cdot sm$ with a thickness of $\sim 4\ \mu m$.

The obtained heterostructures have the most acceptable parameters: no-load voltage and short-circuit current at a temperature of $t_S$ = 400 $^0$C. The n/Si – n/$CdS_xTe_{1-x}$ structures obtained at $t_S$ =465 $^0$C have electrophysical characteristics, in particular volt-ampere characteristics, as in n-i-n- structures with a long base, where d/L = 14-55 (d is a thickness of the i-layer, L is the diffusion length of minority current carriers).

With an increase in temperature $t_S$, the thickness of the $CdS_xTe_{1-x}$ layer increases, and the output parameters of the n/Si – n/$CdS_xTe_{1-x}$ heterostructures deteriorate. Therefore, in this structure, studies were carried out at $t_S$ = 400 $^0$C and 465 $^0$C.

The phase composition of the $CdS_xTe_{1-x}$ solid solution was investigated using the photoelectric method. The spectral distribution of photosensitivity was measured in the valve mode on a ZMR-3 monochromator at room temperature. The radiation source was a DKSSh-1000 xenon lamp with a luminous flux of 53000 lm, brightness up to 120 Mcd/m$^{2,}$ with a central light spot operating in the mode of the minimum allowable power. The radiation is calibrated in absolute units using a thermoelement with an RTE-9 quartz window. The DKSSh-1000 lamp has a continuous spectrum in the UV and visible regions and powerful radiation lines in the near IR region (800-820 nm). In this method, it is important to establish the sizes of the entrance and exit slits and the resolution of the monochromator, which make it possible to correctly measure the parameters of the sample. The performed estimate showed [5] that the slit width should be ~ 10 μm. However, a wider slit was set up in the experiment to ensure sufficient photosensitivity of the sample under study while retaining the possibility of studying subtle phenomena. In this case, the resolution of the monochromator does not exceed 3% in the investigated spectrum region.

## 3 Results and discussion

One of the important issues is the study of the composition of the $CdS_xTe_{1-x}$ solid solution. Figures 1a and 1b show the spectral distributions of the photosensitivity of n/Si – n/$CdS_xTe_{1-x}$ heterostructures obtained for structures grown at substrate temperatures $t_S$ = 400 and 465 $^0$C. In the spectral distribution of photosensitivity between the intrinsic absorption edges of CdS and CdTe for the n/Si – n/$CdS_xTe_{1-x}$ heterostructure obtained at a temperature of $t_S$ = 400 $^0$C, there are clear peaks $\lambda_1^{max}$ = 0.735 μm and $\lambda_2^{max}$ = 0.930 μm (Fig. 1a). The spectral distribution of the photosensitivity of the n/Si – n/$CdS_xTe_{1-x}$ heterostructure obtained at a temperature of $t_S$ = 465 $^0$C has several peaks at $\lambda_1^{max}$ = 0.664 μm, $\lambda_2^{max}$ = 0.692 μm, $\lambda_3^{max}$ = 0.725 μm, $\lambda_4^{max}$ = 0.750 μm, $\lambda_5^{max}$ = 0.788 μm, $\lambda_6^{max}$ = 0.814 μm, $\lambda_7^{max}$ = 0.870 μm, and $\lambda_8^{max}$ = 0.905 μm (Fig. 1b).

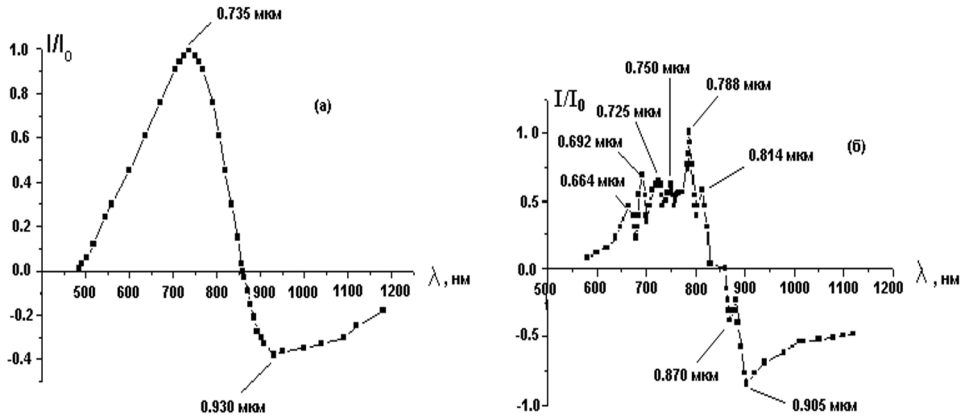


**Fig. 1.** Spectral distribution of photosensitivity of heterojunctions n/Si – n/CdS, grown at temperatures (a) $t_S = 400^0$C and (b) $465^0$C.

For the detected peaks in the spectral dependence of the photosensitivity distribution, the corresponding fundamental absorption edges $\lambda_{c.f.a}$ were determined by extrapolating the long-wavelength edge of the photosensitivity maxima to the λ axis. Using the values of the fundamental absorption edges for the detected peaks in the photosensitivity spectrum, the band gap $E_g$ of solid solutions (SS) formed at the n/Si – n/$CdS_xTe_{1-x}$ heterointerface are determined.

Based on the relationship between the composition of the solid solution and the band gap $E_g(x)$, the composition of the solid solution $CdS_xTe_{1-x}$ was determined for the found values of $E_g$. The determination of the value of the fundamental absorption edge $\lambda_{c.f.a}$, the band gap $E_g$, and the composition $x$ of SS for all detected peaks in the photosensitivity spectrum at $t_S = 400\ ^0$C and $465\ ^0$C are given in Table 1. The values of the lattice constant $a_0$ (x) for the detected solid solutions $CdS_xTe_{1-x}$, which are estimated by the empirical formula $a_0$ (x) [A] = 0.6477−0.0657$x$ [3], are also given in Table 1.

**Table 1.** Dependences of the lattice constant $a_0$ (x), average band gap $E_g^{av}$, and fundamental absorption edges $\lambda_{c.f.a}$ of $CdS_xTe_{1-x}$ solid solution.

| $\lambda_{max}$, nm | $\lambda_{c.f.a.}$, nm | $E_g$, eV | X | $a_0$, (x), Å |
|---|---|---|---|---|
| 664 | 680 | 1.82 | 0.8 | 5.95 |
| 692 | 718 | 1.73 | 0.75 | 5.98 |
| 725 | 755 | 1.64 | 0.69 | 6.02 |
| 750 | 780 | 1.59 | 0.65 | 6.05 |
| 788 | 802 | 1.546 | 0.61 | 6.13 |
| 814 | 830 | 1.53 | 0.56 | 6.158 |
| 735 | 858 | 1.44 | 0.5<br>0.28 | 6.192<br>6.3174 |
| 870 | 881 | 1.407 | 0.45 | 6.2 |

It should be noted that when determining the composition of $CdS_xTe_{1-x}$ solid solutions with $E_g$ = 1.44 eV using the empirical formula $E_g$ [eV] = 1.74$x^2$ – 1.01$x$ + 1.51 [8], the value for $x$ is obtained in the form of two positive values. For other values of $E_g$ of SS, only one positive value for $x$ is obtained. Therefore, in Table 2, for solid solutions with $E_g$ = 1.44 eV, two composition values are given, and for other $E_g$, one value of the composition $x$.

The solid solution with the composition $x$ = 0.8 is closer in composition to the CdS layers, and the solid solution with the composition $x$ = 0.28 is closer to the CdTe layers.

The estimate shows that the value of $a_0$ (x) for Si and SS with a composition of $x$ = 0.8 differ by 8%, and $a_0$ (x) for CdS and SS films with $x$ = 0.8 differ by only 2%.

**Table 2.** Quantitative analysis of chemical components of surfaces of (n/Si-$CdS_xTe_{1-x}$-n/CdS) layers.

| Elmt | Spect. Type | Element % | Atomic % | Elmt | Spect. Type |
|---|---|---|---|---|---|
| Si K | ED | 0.07* | 0.20* | Si K | ED |
| S K | ED | 20.31 | 47.05 | S K | ED |
| Cd L | ED | 78.62 | 49.33 | Cd L | ED |
| Te L | ED | 1.35 | 0.79 | Te L | ED |
| Total | | 100.35 | 100.00 | Total | |

| Element % | Atomic % | Elmt | Spect. Type | Element % | Atomic % |
|---|---|---|---|---|---|
| 0.07* | 0.17* | Si K | ED | 0.03* | 0.09* |
| 22.34 | 50.14 | S K | ED | 22.53 | 50.56 |
| 77.06 | 49.33 | Cd L | ED | 76.74 | 49.14 |
| 0.64 | 0.36 | Te L | ED | 0.39 | 0.22 |
| 100.10 | 100.00 | Total | | 99.69 | 100.00 |

The distribution of chemical elements over the surface of obtained layers is investigated. Analyzes were performed on a Jeol - JXA - 8900 microanalytical complex using an EMF LINK ISIS (energy-dispersive spectrometer); error ± 2.0%. Shooting conditions: V = 20 kV, I = 10 nA. Standards: native Cd, Te, and Si for S - synthetic FeS. The measurement results and the microphotograph are shown in Fig. 2 a) and b).
As shown in Fig. 2b, the emission intensity of the secondary electrons knocked out from the surface layers of the elements of cadmium and sulfide is maximum. This means that the surface of the films mainly consists of cadmium sulfide. The next layer consists of a solid solution of cadmium sulfide and cadmium telluride, then a layer of cadmium telluride and a solid solution of cadmium telluride and silicon.

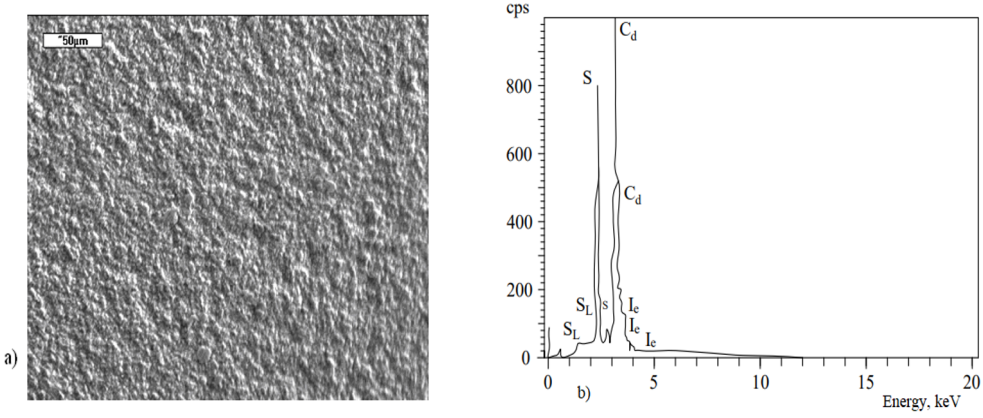


**Fig. 2.** a) microphotograph from surfaces of the layers; b) distributions of chemical elements on surfaces of layers.

Figure 3 *a* and *b* show microphotographs taken from the cleavage of the layers, as well as the dependences of the distribution of chemical elements on the thickness of the layers. The measurement was carried out at several points. The results of studies of the dependence of chemical elements on thickness show that in all measured directions, the distribution of

chemical elements is almost the same, and the average spread is no more than ~ 5%. Figure 3b also shows the dependencies of the layers over the thickness of the films. The topmost microphotograph corresponds to the silicon substrate. The following microphotographs show the distributions of the chemical elements of sulfide, cadmium, and telluride in the layers. From the figure, it is also possible to estimate the respective thicknesses of each composition. For example, the thickness of cadmium sulfide is approximately one-third of the thickness of cadmium telluride (the bump is the third micrograph from the top). The plateau corresponds to the cadmium telluride layer (from the bottom, the second microphotograph on the left side after the crest). Estimating the approximate thickness of solid solutions from the figure (decreases in the plot) is also possible.

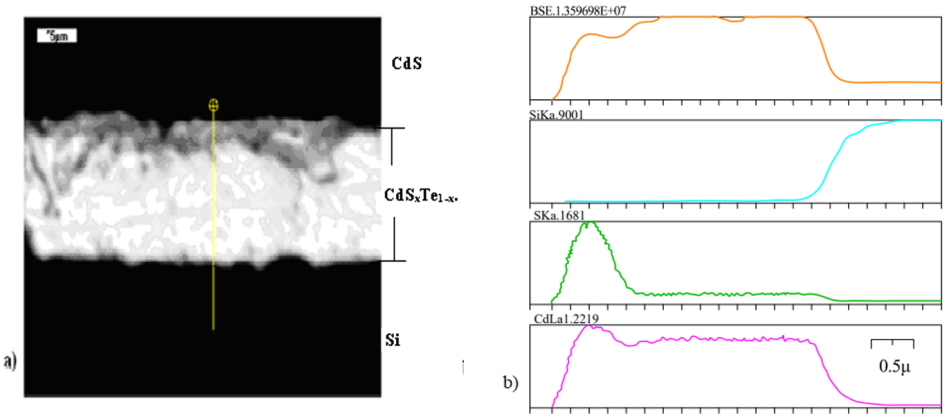


**Fig. 3.** a) microphotographs taken from cleavage of layer; b) course of dependences of distribution of chemical elements on thickness of films.

## 4 Conclusions

Analyzes of the results obtained show that a solid solution between silicon and cadmium telluride, as well as cadmium telluride and cadmium sulfide, is formed with a thickness of ~ up to 2 μm and ~ up to 1 μm, respectively (Fig. 3). According to the authors of [5], based on $A^2B^6$ compounds in the $A^2$ - $B^6$ systems, regions of solid solutions (homogeneity regions) are formed, the length of which can be much larger than that of the $A^3B^5$ compounds. The composition of solid solutions based on $A^2B^6$ compounds can be controlled by setting the conditions for their preparation or processing. Physical and physicochemical properties of solid solutions change with a change in composition, and the nature of the change can be both linear and as well as more complex.

## References

1. A. S. Saidov, A. Yu. Leiderman, Sh. N. Usmonov, and K. T. Kholikov. I–V Characteristic of p–n Structures Based on a Continuous Solid Solution $(Si_2)_{1-x}(CdS)_x$. Semiconductors. Vol. 43(4). pp.416 (2009).
2. A. S. Saidov, Sh. N. Usmonov, K. A. Amonov, Sh. Niyazov and A. I. Khudayberdiyeva. Photothermovoltaic Effect in p-Si–n-$(Si_2)_{1-x-y}(Ge_2)_x(ZnSe)_y$ Structure. Applied Solar Energy. Vol. 55(5). pp. 265–268. (2019).
3. Mirsagatov S. A., Uteniyazov A. K., and Achilov A. S. Mechanism of current transport in Schottky barrier diodes based on coarse-grained CdTe films. Physics of the Solid

State, Vol. 54, pp.1751-1763. (2012).

4. Mirsagatov S. A., and Sapaev I. B. Photoelectric and electrical properties of a reverse-biased p-Si/n-CdS/n+-CdS heterostructure. Inorganic Materials, Vol. 50, pp.437-442. (2014).
5. Mirsagatov S. A., and Sapaev I. B. Mechanism of charge transfer in injection photodetectors based on the M (In)-n-CdS-p-Si-M (In) structure. Physics of the Solid State, Vol. 57, pp.659-674. (2015).
6. Markov V. F., Korotcenkov G., and Maskaeva L. N. Thin Films of Wide Band Gap II-VI Semiconductor Compounds: Features of Preparation. In Handbook of II-VI Semiconductor-Based Sensors and Radiation Detectors: Volume 1, Materials and Technology, pp. 233-275. Cham: Springer International Publishing. (2023).
7. Usmonov S. N., Saidov A. S., and Leiderman A. Y. Effect of injection depletion in p-n heterostructures based on solid solutions (Si 2) 1− x− y (Ge 2) x (GaAs) y,(Si 2) 1− x (CdS) x,(InSb) 1− x (Sn 2) x, and CdTe 1− x S x. Physics of the Solid State, Vol. 56, pp. 2401-2407. (2014).
8. Bonnet D., and Rabenhorst H. Proc. Int. Conf. Physics and Chemistry of Semiconductor Heterojunction and Layer Structure. (1971).
9. Uda H., Sonomura H., and Ikegami S. Screen printed CdS/CdTe cells for visible-light-radiation sensor. Measurement Science and Technology, Vol. 8(1), p. 86. (1997).
10. Kudii D., Meriuts A., Khrypunova A., Shelest T., Varvianska V., and Zaitsev R. Theoretical Analysis of Optical Properties of CdS/CdTe Film Heterosystems. In 2020 IEEE 4th International Conference on Intelligent Energy and Power Systems (IEPS) (pp. 135-139). IEEE. (2020).